

Morphogenic Effect of Solvent on Crew-Cut Aggregates of Amphiphilic Diblock Copolymers

Yisong Yu, Lifeng Zhang, and Adi Eisenberg*

Department of Chemistry, McGill University, 801 Sherbrooke Street West, Montreal, Quebec, Canada H3A 2K6

Received August 19, 1997; Revised Manuscript Received November 24, 1997

ABSTRACT: It is shown that the morphologies and other characteristics of crew-cut aggregates of polystyrene-*b*-poly(acrylic acid) (PS-*b*-PAA) diblock copolymers are related to the nature of the initial common solvent in which the micelle-like aggregates are prepared. Polymer-solvent interactions determine the dimensions of both the core and the corona of the aggregates. Solubility parameters and dielectric constants of the solvents can be used to estimate the strength of the PS-solvent interaction (which influences the solvent content in the core) and the strength of PAA-solvent interaction (which influences the repulsion among corona chains). The closer the match between the solubility parameter of the solvent and that of the core forming block, the higher the solvent content of the core and the higher the degree of stretching of the core chains. The lower the polarity of the solvent, the weaker the PAA-solvent interaction and the weaker the repulsive interactions among the corona chains; this increases the aggregation number and degree of stretching in the core. As the degree of stretching of PS chains in the cores increases and the repulsion among the corona decreases, the morphology of the aggregates can change progressively from spheres to cylinders, to vesicles, or to large compound micelles. In *N,N*-dimethylformamide, the core dimensions are smaller and the corona dimensions are larger than in tetrahydrofuran (THF) or dioxane, so spherical aggregates are favored. In THF, the solvent content in the core and the corona dimension are larger than in dioxane. Since an increase of solvent content in the core favors a morphological change away from spheres, but a larger corona dimension favors spheres, the final morphology is determined by a balance of these two factors. Relationships between the nature of common solvent and critical water content as well as degree of micellization are studied in detail. Finally, morphological changes for the same diblock copolymer in different solvents are explored further.

1. Introduction

The self-assembly of amphiphilic diblock copolymers in selective solvents generally results in aggregates of a core-shell structure.^{1–3} In parallel with small molecule systems, when the hydrophobic block is in the core and the hydrophilic block in the corona, the aggregates, in aqueous media, are referred to as regular micelles;^{4–18} by contrast, aggregates which have a hydrophilic core and a hydrophobic corona, in nonaqueous media, are called reverse micelles.^{19–22} When the dimensions of the corona are large relative to those of the cores, the aggregates are referred to as star micelles;^{1–9,19} When the core is bulky and the corona is relatively short, the aggregates are called “crew-cut”.^{10–18,20–22}

Aggregates with a spherical morphology have been identified in many block copolymer solutions.^{1–10,19} They consist of a core formed by the insoluble blocks and a corona formed by the soluble blocks. In most cases, only such aggregates are obtained if the soluble block is long relative to the insoluble block. Nonspherical or bilayer aggregates in solutions of block copolymers were observed only rarely, and mostly indirectly; this has been reviewed in a previous paper.¹²

It is only quite recently that the crew-cut aggregates with nonspherical or bilayer morphologies have received extensive attention.^{12–18,20–22} These are prepared very differently from the methods used for star micelles, which are usually made directly by dissolving a highly asymmetric block copolymer in a selective solvent which is good for the long corona block. In the course of the

dissolution, the insoluble short blocks form the core and the soluble long blocks form the corona of the micelles. However, it is difficult to prepare crew-cut aggregates by this method because the insoluble block is too long and the soluble block is too short for the direct formation of such structures. Therefore, to prepare crew-cut aggregates from highly asymmetric diblock copolymers of, for example, polystyrene and poly(acrylic acid) (PS-*b*-PAA), with relatively long PS blocks and relatively short PAA blocks in aqueous solution,¹² the diblock copolymers are first dissolved in a common solvent (e.g., *N,N*-dimethylformamide (DMF)) and then a precipitant (e.g., water) is added to the polymer solution. As the addition of water progresses, the quality of the solvent for the PS block decreases gradually. The micellization of the PS block chains starts when the water content reaches a critical point (critical water content or cwc). More water is added and the DMF is removed from the aggregates by dialyzing the colloidal solution against water.

PS-*b*-PAA crew-cut aggregates with various morphologies, such as spheres, rods, lamellae, vesicles, and large compound micelles consisting of aggregates of reverse micelles with a hydrophilic surface, can be obtained by the method mentioned above.¹² When the PAA content in the block copolymer is relatively high, the diblock copolymer yields spherical micelle-like aggregates. In contrast to star micelles, the crew-cut micelles have a low density of coronal chains on the core surface and a low degree of stretching of the PS chains in the core. As the PAA content decreases, the morphology of the aggregates changes from spheres to cylinders, to bilayers, and eventually to large compound micelles. Other

* To whom correspondence should be addressed. E-mail: eisenber@omc.lan.mcgill.ca.

morphologies, such as tubes, "pincushions", and large compound vesicles, have also been described very recently.¹⁴

Crew-cut aggregates of various morphologies have also been obtained from polystyrene-*b*-poly(ethylene oxide) (PS-*b*-PEO) diblock copolymers, which are completely nonionic.¹⁴ Subsequently, it was shown that aggregates of multiple morphologies can be obtained from polybutadiene-*b*-poly(acrylic acid) (PBD-*b*-PAA) diblocks, which have cores with glass transition temperatures (T_g) in the range of -90 to -8 °C (i.e., far below room temperature at which the aggregates are formed and studied).¹⁵ Aggregates of multiple morphologies can also be prepared in organic solvents, in which the more hydrophobic or more soluble blocks form the corona.^{21,22}

In the early stages of aggregation, a thermodynamic equilibrium is operative between the unimers and the aggregates. Under such conditions, the aggregates should strictly be called micelles. As more water is added and more solvent is progressively extracted from the aggregate cores, the structures of the aggregates become kinetically frozen.¹⁷ For convenience, we use term of aggregates to refer to the colloidal particles formed under equilibrium condition (early stage) and subsequently frozen (late stage) as more water is added. Because the exploration of crew-cut aggregates started only very recently, many aspects related to their formation mechanism are still not clear. Generally, from a thermodynamic point of view, the structures of the crew-cut aggregates are considered to be controlled mainly by three contributions to the free energy of micellization, (i.e., the stretching entropy of the core-forming blocks, the repulsive interaction among the corona chains, and the interfacial tension at the core-corona interface.¹² The morphogenic effect of changing the interaction among the corona chains on the aggregates has been evidenced both by changing the polymer compositions and by the addition of ions.^{12,13} The effect of added ionic species on the aggregate morphology is similar to that of changing block copolymer composition.¹³ The repulsion among the PAA corona chains is modified by the addition of NaCl, HCl, or CaCl₂ due to changes of electrostatic screening, protonation, and ion binding. As a result, the force balance is changed, which induces the formation of aggregates with multiple morphologies from an identical block copolymer. The morphology of the aggregates is also related to the initial polymer concentration in the solutions.¹⁶

For a compact PS aggregate core, some of the PS core-forming blocks must span the distance from the core/corona interface to the core center. As the dimension of the aggregates changes, the extent to which the PS chains are stretched in the aggregate core changes. An increase of the degree of stretching of PS chains in the aggregate core results in a decrease of the entropy of the PS chains. Nagarajan²³ theoretically predicted that the amount of solvent in the aggregate core can effect the morphology of the aggregates. For a given copolymer composition, the preferred structure at the solvent content under consideration is the structure associated with the lowest optimal free energy of solubilization. As the degree of solubilization (solvent content) in the core increases, the morphology of aggregates changes from spheres, to rods, and then to vesicles. It is obvious that when the solvent content in the aggregate core increases, the dimension of the core must increase,

resulting in an increase of the degree of stretching of the core-forming chains.

One way of changing the core dimension which has not yet been explored is to change the solvent and thus to take advantage of the wide range of accessible polymer-solvent interaction parameters. The amount of solvent in the aggregate cores during micellization is related to the thermodynamics of the interaction between the solvent and the core-forming block. The stronger the interaction, the more solvent is in the core. Polymer-solvent interactions affect not only the core dimension, but also repulsive interaction among the corona chains. In a very recent preliminary communication,²⁴ we reported that solvent-induced changes in the core dimension have, indeed, a major effect on the morphology of crew-cut aggregates of amphiphilic block copolymers. Aggregates of various morphologies could be prepared from a single quaternized polystyrene-*b*-poly(4-vinylpyridine) block polyelectrolyte or a polystyrene-*b*-poly(acrylic acid) diblock copolymer by only changing the common solvent.

In the present paper, we report on the detailed study of the effect of the common solvent on the morphology of the diblock copolymers of polystyrene-*b*-poly(acrylic acid). In particular, we report the relationship between the degree of micellization and the nature of the common solvent, as well as the dependence of the aggregate structure on the compositions of the common solvents. Finally, the morphogenic effect of the solvent is attributed to the relative strength of polymer-solvent interaction. The PS-solvent interaction strength is related to the solvent content in the core and its effect on the degree of stretching of the PS chains, while the PAA-solvent interaction strength is related to the repulsion among the corona chains. The morphology of aggregates is determined by a combination of both influences.

2. Experimental Section

2.1. Polymer Samples. Polystyrene-*b*-poly(*tert*-butyl acrylate) (PS-*b*-PtBuA) diblock copolymers were synthesized by sequential anionic polymerization of styrene and *tert*-butyl acrylate in tetrahydrofuran (THF) with *sec*-butyllithium as initiator. LiCl and α -methylstyrene were used to prevent side reaction from *tert*-butyl acrylate polymerization.²⁵ Polymerizations were carried out under a nitrogen atmosphere in a round-bottomed flask equipped with a rubber septum. Solvents, initiators, and monomers were transferred via a stainless capillary and syringe to the reactor. *Sec*-butyllithium was first added into the glass reactor containing the LiCl and α -methylstyrene (both were in 10-fold excess relative to the *sec*-butyllithium) in THF; a dark red color appeared. After the temperature was decreased to -20 °C, the styrene was added, turning the color to orange; the polymerization of styrene was completed in a few minutes, and the dark red color returned. An aliquot of the reaction medium was withdrawn to obtain a sample of the homopolystyrene for size exclusion chromatography to determine the block length of polystyrene. The polymerization solution was cooled to -78 °C; as soon as the *tert*-butyl acrylate was added into the reactor, the red color disappeared completely; the polymerization of the *tert*-butyl acrylate was carried out for 30 min; methanol was used to terminate the anionic polymerization. The poly(*tert*-butyl acrylate) block in the block copolymer was hydrolyzed to its acid form, poly(acrylic acid), in toluene at 110 °C by refluxing overnight in the presence of *p*-toluenesulfonic acid as the catalyst. A detailed description of the procedure can be found elsewhere.²⁶

The degree of polymerization of homopolystyrene (homo-PS) and the polydispersity of the homo-PS and PS-*b*-PtBuA diblock

Table 1. Molecular Characteristics of Homopolystyrene and of Polystyrene-*b*-poly(acrylic acid) Diblock Copolymers

polymer ^a	PAA content (mol %)	M_w/M_n^b
PS ₂₀₀	0	1.05
PS ₁₆₈ - <i>b</i> -PAA ₅₉	26.0	1.09
PS ₄₉₀ - <i>b</i> -PAA ₈₇	15.1	1.08
PS ₅₀₀ - <i>b</i> -PAA ₅₈	10.4	1.04
PS ₃₉₀ - <i>b</i> -PAA ₄₁	9.5	1.06
PS ₂₀₀ - <i>b</i> -PAA ₁₈	8.3	1.05
PS ₄₂₀ - <i>b</i> -PAA ₃₂	7.1	1.05
PS ₄₂₀ - <i>b</i> -PAA ₂₆	5.8	1.05
PS ₄₂₀ - <i>b</i> -PAA ₂₁	4.8	1.05

^a Degree of polymerization of the polystyrene was determined by SEC; the poly(acrylic acid) chain length determined by FTIR relative to that of the PS block. ^b Polydispersity index, measured by SEC, of polystyrene or of the whole diblock copolymer in the form of PS-*b*-PtBuA.

copolymers were analyzed by size exclusion chromatography (SEC). The degree of polymerization of the poly(*tert*-butyl acrylate) block was calculated from the polymer composition, which had been determined by Fourier transform infrared (FTIR) spectroscopy.²⁶ All of the homopolymers and block copolymers had narrow and monomodal molecular weight distributions. The molecular parameters of the polymers are listed in Table 1. The polymers are denoted as PS_{*x*} or PS_{*x*}-*b*-PAA_{*y*}, where *x* and *y* stand for the number average degrees of polymerization of the PS and PAA blocks, respectively. For example, PS₂₀₀-*b*-PAA₁₈ represents a diblock copolymer containing 200 styrene units and 18 acrylic acid units.

2.2. Static Light Scattering. Light-scattering measurements were carried out on a DAWN-F multiangle laser photometer (Wyatt Technology, Santa Barbara, CA) equipped with a He-Ne Laser (632.8 nm). The polymer solutions were prepared by dissolution of the polymers in a common solvent (i.e., *N,N*-dimethylformamide (DMF), tetrahydrofuran (THF), or 1,4-dioxane). The solvents DMF, THF, and dioxane (Aldrich, HPLC grade) were used as received without further purification. All solutions were filtered through a membrane filter with a nominal pore size of 0.45 μm. Deionized water (Milli Q) was added with a microsyringe. All measurements were carried out at room temperature. The scattered light intensity was recorded 15 min after each addition of water and mixing of the solution.

2.3. Preparation of the Aqueous Solutions. To prepare the colloidal solutions, deionized water, as a precipitant, was added at a rate of 0.3 wt %/10 s with vigorous stirring to the copolymer solution in the common solvent. For example, for PS₂₀₀-*b*-PAA₁₈ at a concentration of 0.5 wt %, micellization occurred at a water content of approximately 5 wt % in DMF, 11 wt % in 1,4-dioxane, and 18 wt % in tetrahydrofuran (THF). When a mixture of solvents was used, the critical water content for micellization was a function of the solvent composition. More water was added until the water content reached ca. 50 wt %. Finally, the organic solvents are removed by dialysis of the colloidal solutions against pure water for 3 days.

2.4. Transmission Electron Microscopy. Transmission electron microscopy (TEM) was carried out on a Philips EM410 microscope operating at an acceleration voltage of 80 kV. Aqueous aggregate solutions free of organic solvents were used to make the TEM samples. A drop of a very dilute solution was placed onto a copper EM grid, which had been precoated with a thin film of Formvar and then coated with carbon. A few minutes after the deposition, the aqueous solution was blotted away with a strip of filter paper. After drying in air for a few hours, the grids were shadowed with palladium/platinum alloy at an angle of ca. 30°.

2.5. Solvent Content in the PS-Rich Phase. Homopolystyrene (homo-PS) was dissolved in various solvents, i.e., DMF, dioxane and THF, at a concentration of 2 wt %; a given amount of water was then added slowly to a point beyond the critical water content (cwc) at which phase separation occurred. After a waiting period of ca. 1 day, the PS-rich phase settled to the

bottom of the container, and the two phases were easily separated. The solvent content in the polymer-rich phase is defined as the volume ratio of the solvent in the PS-rich phase to the total PS-rich phase. The volume of total PS-rich phase was measured directly, and the volume of the solvent in the PS-rich phase was calculated by recovering the PS from the PS-rich solution after solvent evaporation.

3. Results and Discussion

The Results and Discussion section consists of three parts. First, we describe the quantitative relationship between the precipitation of homopolystyrene or the micellization of polystyrene-*b*-poly(acrylic acid) (PS-*b*-PAA) diblock copolymers and the nature of the initial common solvent, as determined by light-scattering measurements. In part two, the relationship between the nature of the common solvent and the aggregate morphology, as determined by TEM, is presented. Finally, the reasons for the morphogenic effect of the solvent on the PS-*b*-PAA aggregates are related to the strength of the polymer-solvent interactions.

3.1. Micellization of Polymers. The micellization of polystyrene-*b*-poly(acrylic acid) (PS-*b*-PAA) diblock copolymers in solution was observed by static light scattering. DMF, THF, and dioxane are well-known common solvents for both blocks of the PS-*b*-PAA copolymers; thus, the polymer chains are unimolecularly dispersed in the solutions. Since water is a good solvent only for the PAA blocks, the solvent quality becomes progressively worse for the PS as water is added to the copolymer solution in the common solvent. At some point of water addition, the PS block starts to associate and microphase separation occurs. As a result, the scattered light intensity increases suddenly and the solution appears cloudy.

3.1.1. Critical Water Content of the Polymers in Various Solvents. The critical water content (cwc) of a polymer solution is defined as the water content at which micellization starts. The cwc values are usually obtained by observation of the onset turbidity of the polymer solutions or by light-scattering measurements. The cwc values of homopolystyrene and of the PS-*b*-PAA diblock copolymers in DMF have been reported in a previous paper.¹⁷ It was found that the cwc depends on both the polymer concentration and the molecular weight. The higher the copolymer concentration and the molecular weight of the PS blocks, the lower the cwc. The cwc values of homopolystyrene and the PS-*b*-PAA diblocks in DMF are normally in the range of 2–9 wt %.¹⁷ It is well-known that the solubility of the polymer is related to the nature of the solvent. In the present study, THF and dioxane were used as initial common solvents, and the cwc results were compared with those for DMF. Figure 1 presents the experimental curves of the scattered light intensity from homopolystyrene PS₂₀₀ and PS₂₀₀-*b*-PAA₁₈ diblock copolymer in the three solvents as a function of the water content. When the water content is low, the scattered light intensity is almost constant. However, when the water content reaches some critical value, the scattered light intensity increases rapidly. The increase in the scattered light intensity indicates that micellization has taken place. For each solution, a critical water content is obtained from the intercept of the nearly horizontal and vertical straight line segments of the scattered light intensity curves. The critical water contents of both homopolystyrene and PS-*b*-PAA diblock copolymer are related to the nature of the common solvent, and decrease from

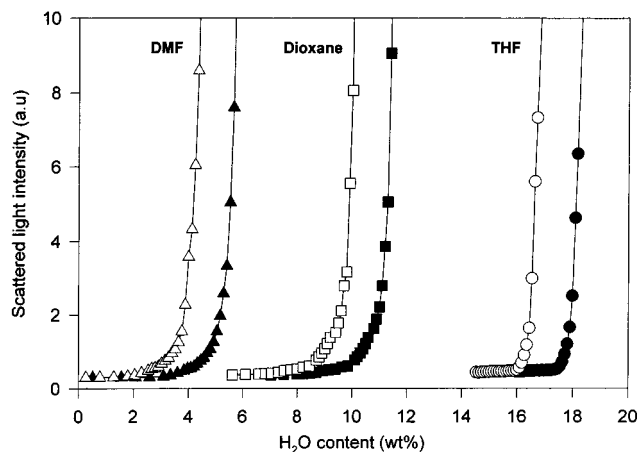


Figure 1. Scattered light intensity as a function of added water content for PS₂₀₀ (open symbols) and PS₂₀₀-b-PAA₁₈ (filled symbols) in various solvents (the initial polymer concentration was 0.5 wt % for all experiments).

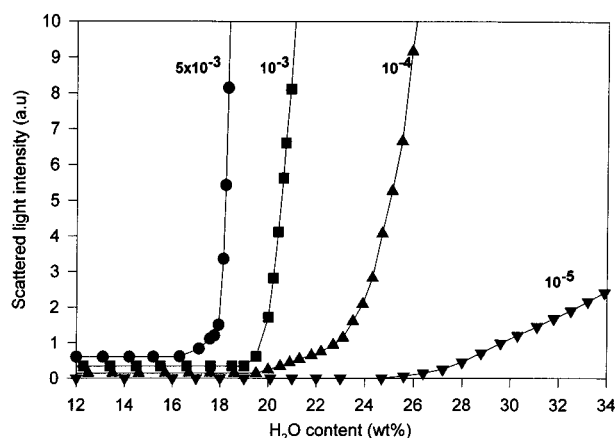


Figure 2. Scattered light intensity as a function of added water content in PS₂₀₀-b-PAA₁₈ solution in THF at different concentration.

THF, to dioxane, and then to DMF. The critical water content of homopolystyrene is only slightly lower than that of the PS-*b*-PAA diblock copolymer in the same solvent, because the major component of the block copolymer is polystyrene. Figure 1 clearly indicates that the polystyrene chains remain soluble to a much higher water content in THF solutions (ca. 18 wt %) compared to DMF solutions (ca. 5 wt %).

3.1.2. Effect of Polymer Concentration on the Critical Water Content in Various Solvents. Figure 2 shows the experimental plot of the scattered light intensity as a function of the water content from PS₂₀₀-b-PAA₁₈ copolymer in THF at various concentrations. In parallel with the behavior in DMF,¹⁷ the onset of the micellization shifts to higher water contents as the initial polymer concentration decreases.

Figure 3 shows a plot of the cwc as a function of the polymer concentration for the same copolymer in the three solvents. A linear relationship is found between the cwc and the logarithm of the polymer concentration; the cwc value decreases as the polymer concentration increases. The cwc in THF is highest, and that in DMF is lowest. As might be expected, the slope of the plot of cwc vs the logarithm of the polymer concentration differs for the different solvents.

3.1.3. Micelle Fraction of PS-*b*-PAA in Various Solvents. As more and more water is added to the

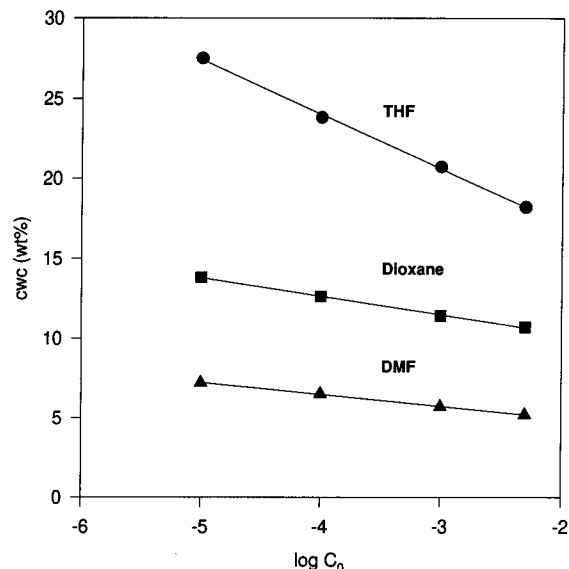


Figure 3. Critical water content vs logarithm of the polymer concentration for a solution of PS₂₀₀-b-PAA₁₈ diblocks in various solvents.

polymer solution beyond the cwc, more and more polymer chains associate to form micelles, and the concentration of the copolymers in single-chain form decreases. A relationship between the micelle fraction of PS-*b*-PAA in DMF and the water content has been given in a previous paper.¹⁷ The micelle fraction is defined as the ratio of the associated polymer to the total polymer, $(C_0 - C_{cmc})/C_0$ (where C_0 stands for the initial polymer concentration and C_{cmc} for critical micellization concentration). In that solvent, the micelle fraction was found to increase rapidly within a very narrow range of water contents once microphase separation started. The relationship between the micelle fraction and the water content is naturally expected to depend on the nature of the common solvent, since the relationship between the cwc and the polymer concentration is related to the nature of the common solvent as shown in Figure 3.

The micelle fraction can be calculated using the following relationship:¹⁷

$$(C_0 - C_{cmc})/C_0 = 1 - \exp(-2.303\Delta H_2O/A)$$

where ΔH_2O is the increment of the water content above the cwc and A is obtained from the slope $d[\text{cwc}]/d[\log C_0]$ in Figure 3. When the ΔH_2O value is zero or less (i.e., for water contents below the cwc), the $(C_0 - C_{cmc})/C_0$ is zero and all the copolymer chains in the solution are unassociated.

A plot of the micelle fraction against the increment of the water content in various solvents is shown in Figure 4, with the insert showing the plot against absolute values of the water content. In DMF or dioxane, the micelle fraction increases very rapidly relative to THF. For 99.5% micellization in each solvent, the calculated water increments beyond the cwc are 1.66 wt % in DMF, 2.63 wt % in dioxane, and 7.48 wt % in THF. These data indicate that the effect of water content on the micellization in THF solution is weaker than that in DMF or in dioxane. The above results also confirm that for all of the solvents, the micellization is complete when the water content is far below 50 wt %, the point at which water addition is

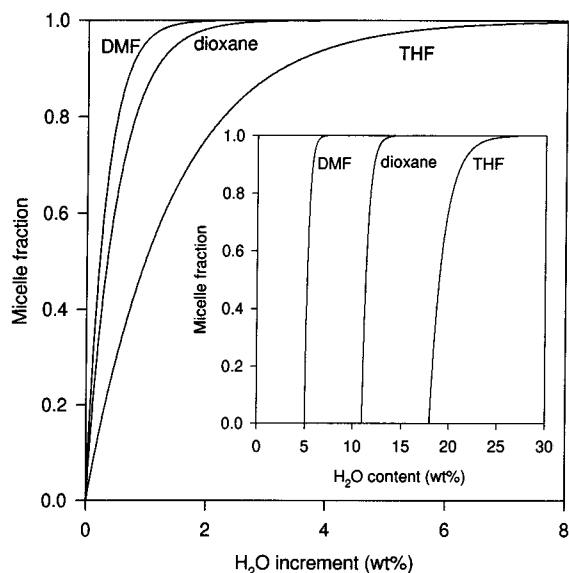


Figure 4. Micelle fraction as a function of water increment beyond the critical water content (PS₂₀₀-*b*-PAA₁₈, 0.5 wt %). The insert shows the plot against the absolute water content.

Table 2. Aggregate Morphologies of PS-*b*-PAA Diblocks in Different Common Solvents (the Initial Polymer Concentration was 2 wt %)

polymer	PAA content (mol %)	DMF	dioxane	THF
PS ₁₆₈ - <i>b</i> -PAA ₅₉	26.0	sphere	sphere	sphere
PS ₄₉₀ - <i>b</i> -PAA ₈₇	15.1	sphere	rod	sphere
PS ₅₀₀ - <i>b</i> -PAA ₅₈	10.4	sphere	vesicle	vesicle
PS ₃₉₀ - <i>b</i> -PAA ₄₁	9.5	sphere	vesicle	vesicle
PS ₄₂₀ - <i>b</i> -PAA ₃₂	7.1	sphere	vesicle	LCM
PS ₄₂₀ - <i>b</i> -PAA ₂₆	5.8	sphere	vesicle	LCM
PS ₄₂₀ - <i>b</i> -PAA ₂₁	4.8	sphere	LCM	LCM

stopped prior to dialysis (see Experimental Section). Therefore, the single-chain content in the solution is negligible for the conditions under which all of the experiments were performed.

3.2. Morphogenic Effect of Solvent on PS-*b*-PAA Aggregates. It has been reported that the morphology of the PS-*b*-PAA crew-cut aggregates is controlled by several factors (i.e., the polymer composition and concentration, the presence of ions, etc.^{12,13,16}). However, all of these methods are limited to a relatively narrow range of polymer compositions. For example, when the PAA content is higher than 10 mol % (for a PS chain of 400 repeat units), morphologies other than spheres have not been obtained in DMF, regardless of any changes in the polymer concentration or the addition of ions. In the present study, it has been found that when the common solvent is changed from DMF to dioxane or THF, the range of polymer compositions in which nonspherical morphologies are seen is extended to a much broader range of PAA contents. Table 2 illustrates the relationship between the morphology of PS-*b*-PAA aggregates and the nature of the common solvent for several diblocks of different compositions.

3.2.1. Morphologies of PS-*b*-PAA Crew-Cut Aggregates from Dioxane. All the PS-*b*-PAA diblock copolymers studied here yield only spherical aggregates in DMF at a concentration of 2 wt %. In contrast, the aggregates prepared from dioxane show the entire range of morphologies. Figure 5 shows a set of typical TEM pictures of the aggregates made from these diblocks in dioxane. Figure 5A shows spherical aggregates made

from PS₁₆₈-*b*-PAA₅₉ (26.0 mol % PAA). The average diameter of the spheres is *ca.* 32 nm. As usual, the polydispersity of the diameters is low. Aggregates with a cylindrical morphology are obtained when the PAA content decreases to 15.1 mol % (PS₄₉₀-*b*-PAA₈₇). Figure 5B shows a typical example. Most of the aggregates appear to be straight rather than bent cylinders. These cylinders have relatively uniform diameter (*ca.* 57 nm) but differ widely in length. Hemispherical caps are clearly seen at the cylinder ends. Some spheres are still present. As the ratio of PAA to PS block lengths drops further, vesicles are formed (Figure 5C–E), with sizes increasing as the PAA content decreases. PS₅₀₀-*b*-PAA₅₈ (10.4 mol % PAA) yields small vesicles (Figure 5C). The vesicular nature is evidenced from a higher transmission in the center of the aggregates than around their periphery, in combination with the height measurements from shadowing which suggests that the aggregates are spherical. The outer diameters range from 100 to 150 nm, and the average wall thickness is *ca.* 37 nm. As PAA content decreases to 9.5 mol % (PS₃₉₀-*b*-PAA₄₁), the outer diameters increase to the range of 150–500 nm, and the average wall thickness is *ca.* 39 nm (Figure 5D). With a further decrease of the PAA content to 5.8 mol % (PS₄₂₀-*b*-PAA₂₆), elliptical vesicles of very large sizes can form (Figure 5E). When the PAA block length becomes still shorter (PS₄₂₀-*b*-PAA₂₁), aggregates consisting of large solid spheres of high polydispersity are obtained. These aggregates are probably large compound micelles consisting of an assembly of reverse micelles with a hydrophilic surface, as described previously.¹²

3.2.2. Morphologies of PS-*b*-PAA Crew-Cut Aggregates from THF. Table 2 shows that spheres, vesicles, and LCMs can be obtained in THF over the range of compositions studied here. Two characteristics are worth noting. First, morphologies other than small spherical aggregates or LCMs form only in a relatively narrow range of PAA contents in THF (upper limit between 10.4 and 15.1 mol % and lower limit between 7.1 and 9.5 mol % PAA) relative to that in dioxane (upper limit between 15.1 and 26.0 mol % and lower limit between 4.8 and 5.8 mol % PAA). Second, rodlike aggregates are not seen in THF. Two possible explanations can be suggested for the absence of rods. First, the composition range for the formation of these aggregates might be very narrow, and no samples have been prepared within this range. Second, it is possible that in THF, the morphology changes directly from spheres to vesicles. Nagarajan²³ has predicted theoretically the existence of two types of mechanisms for the morphological transition from small spheres to vesicles. One mechanism involves spheres, rods, and bilayers, while only spheres and bilayers are expected from the other.

3.2.3. Aggregate Morphology of an Identical PS-*b*-PAA Diblock in Mixtures of DMF and THF. The solvent effect becomes a versatile tool of morphological control when a mixture of solvents is used. Table 2 shows that the same PS-*b*-PAA diblock copolymer can yield different morphologies in different solvents. It is therefore of interest to inquire whether a progressive change in the nature of the common solvent (as a result of mixing) is accompanied by gradual changes in the aggregate morphology. The following study was performed to answer this question.

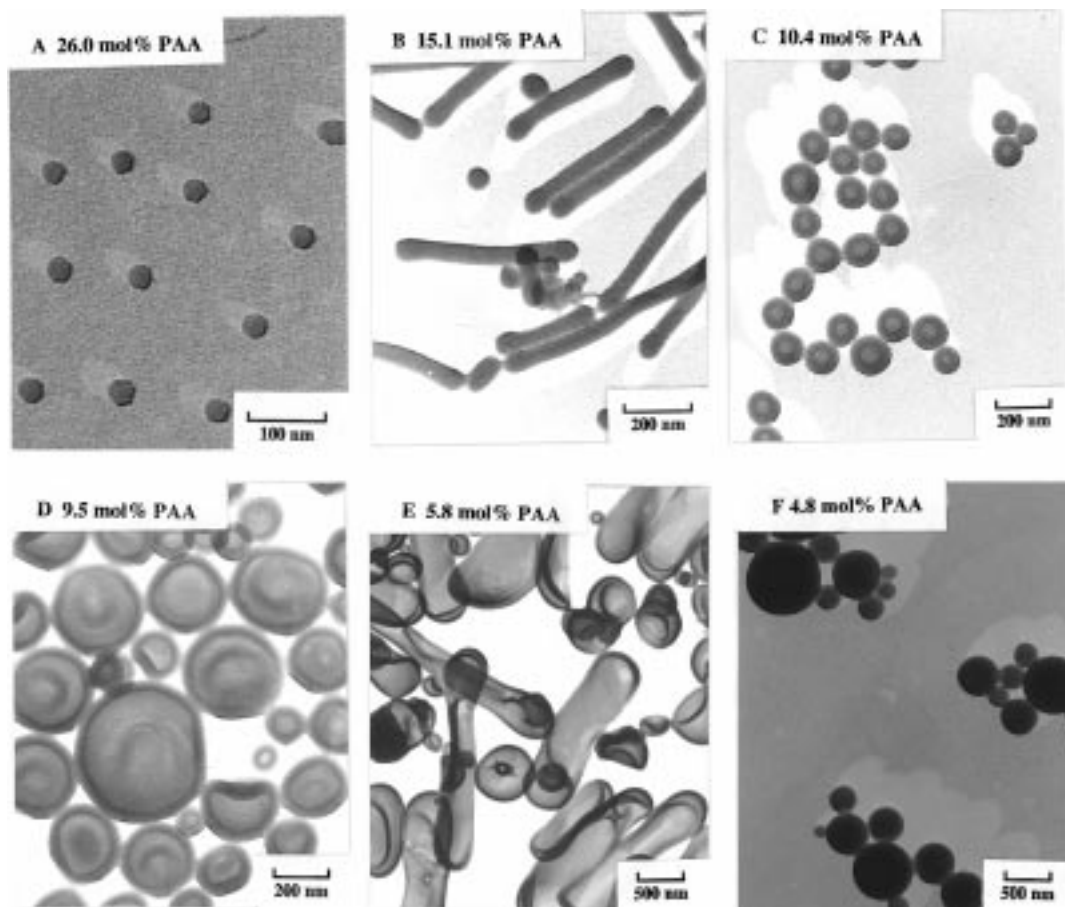


Figure 5. TEM pictures of PS-*b*-PAA crew-cut aggregates made in dioxane: (A) PS₁₆₈-*b*-PAA₅₉; (B) PS₄₉₀-*b*-PAA₈₇; (C) PS₅₀₀-*b*-PAA₅₈; (D) PS₃₉₀-*b*-PAA₄₁; (E) PS₄₂₀-*b*-PAA₂₆; (F) PS₄₂₀-*b*-PAA₂₁ (the initial polymer concentration was 2 wt %).

PS₂₀₀-*b*-PAA₁₈ yields spherical aggregates in DMF (Figure 6A) and large compound micelles (LCMs) in THF (Figure 6H). Figure 6B–G show that with increasing THF content in the solvent mixture (the initial polymer concentration before the addition of water is 0.5 wt % for all experiments), the morphology of the PS-*b*-PAA crew-cut aggregates changes progressively from spheres in 0 wt % THF (Figure 6A), to interconnected rods in 5 wt % THF (Figure 6B), to a mixture of rods, lamellae, and vesicles in 10 wt % THF (Figure 6C), to only small vesicles in 25 wt % THF (Figure 6D), to medium-sized vesicles in 40 wt % THF (Figure 6E), to larger vesicles in 50 wt % THF (Figure 6F), to a mixture of vesicles and LCMs in 67 wt % THF (Figure 6G), and finally to LCMs in pure THF (Figure 6H).

The aggregates shown in Figure 6 are now discussed briefly. The spherical micelles (Figure 6A) have an average diameter of *ca.* 30 nm and a low polydispersity. The aggregate solution prepared in 5 wt % THF/95 wt % DMF (Figure 6B) shows a bluish color, and gellike pieces are seen to be suspended in the solution. They appear to consist of interconnected rods. Only a few ends are free, and these contain hemispherical caps. The average diameter of the rods is *ca.* 27 nm.

When the THF content is raised to 10 wt %, the aqueous solutions become slightly cloudy. A mixture of rods, lamellae, and vesicles is seen in the solution (Figure 6C). The lamellar nature is evidenced by the uniformity of the light intensity over the entire feature in the micrograph. The thickness of the lamellae (as judged from the length of the shadowed region), the diameter of rods and the wall thickness of the

vesicles are the same; the average value is *ca.* 23 nm.

When the THF contents are in the range of 25–67 wt %, vesicles are observed and the solutions are turbid. The outer sizes and the wall thicknesses of the vesicles are found to increase with increasing THF content. Figure 6D shows a typical example of the vesicles obtained from 25 wt % THF. These vesicles have a outer diameter of *ca.* 80 nm and a relatively low polydispersity. The average wall thickness is *ca.* 29 nm. When the THF concentration is further increased to 40 wt %, the sizes of vesicles increase and the polydispersity broadens. Figure 6E shows a typical example. The sizes now are in the range of 70–200 nm, but the wall thickness is still very uniform, at *ca.* 30 nm. The sizes of vesicles are further increased when the THF content is raised to 50 wt %, as shown in Figure 6F. They now have diameters in the range of 300–500 nm. The average wall thickness is now *ca.* 36 nm, but in some cases, the wall thickness is double (i.e., *ca.* 70 nm). These vesicles with a double wall thickness are believed to be bilamellar vesicles, one trapped inside the other. However, for most of the trapped vesicles, which are seen quite frequently, the sizes of inner and outer vesicles are very different. When the THF content is 67 wt % (Figure 6G), vesicles are still the dominant aggregates, but LCMs can be seen occasionally. The sizes of vesicles are in the range of 300–600 nm. The average wall thickness of the vesicles is *ca.* 39 nm. With a further increase in the THF content, the percentage of vesicles decreases and that of the LCMs increases, until only LCMs are seen in pure THF (Figure 6H).

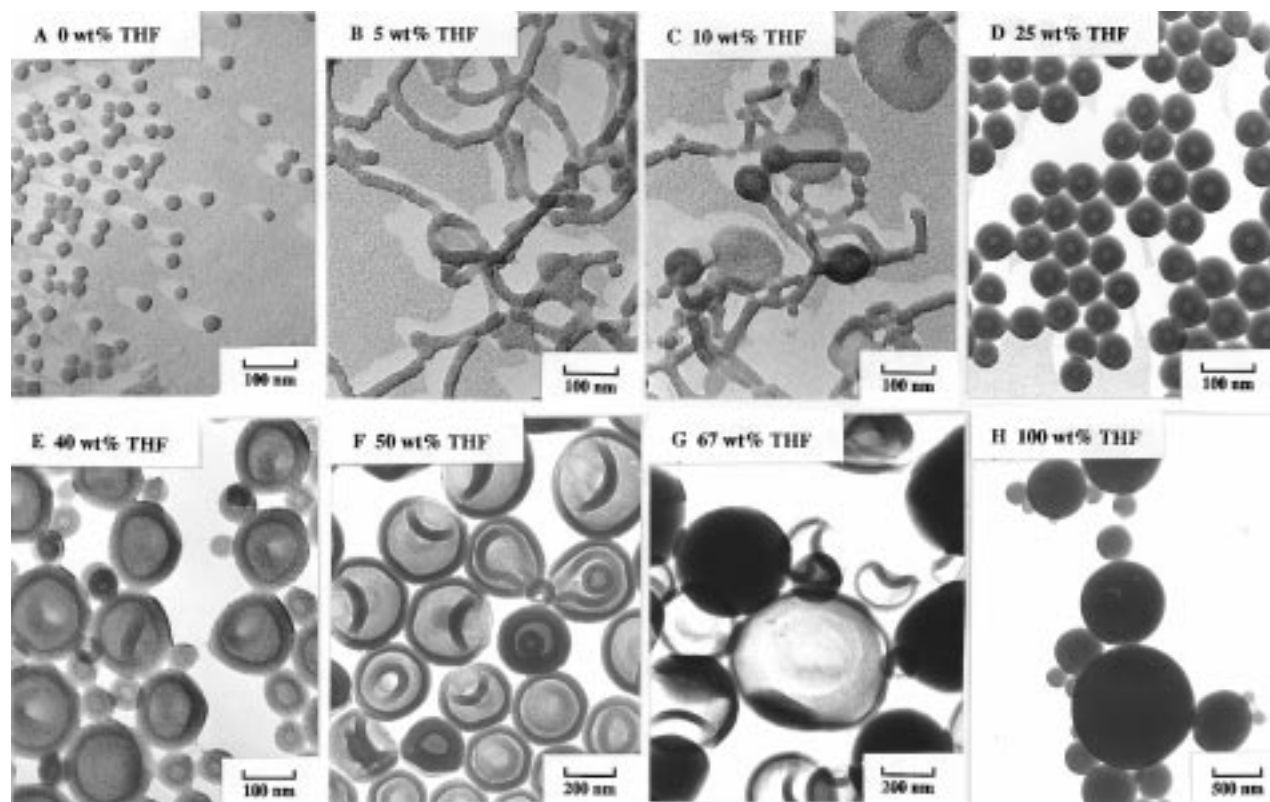


Figure 6. TEM pictures of PS₂₀₀-*b*-PAA₁₈ crew-cut aggregates in various mixtures of THF and DMF: (A) 0 wt % THF; (B) 5 wt % THF; (C) 10 wt % THF; (D) 25 wt %; (E) 40 wt % THF; (F) 50 wt % THF; (G) 67 wt %THF; (H) 100 wt %THF (the initial polymer concentration was 0.5 wt %).

Obviously, the morphology of the aggregates changes progressively, corresponding to the composition of the common solvent. The above result suggests a general way to prepare aggregates with various morphologies; when a diblock copolymer yields spherical aggregates in one common solvent and LCMs in another, the entire range of morphologies may be obtained by using mixtures of these two solvents.

3.2.4. Tubular Morphology of PS-*b*-PAA Aggregates from a Mixture of DMF and Dioxane. Much attention has been paid recently to the preparation and characterization of tubules from small molecule amphiphiles because of potential applications as well as the biomimetic nature of the tubules. These tubules tend to be structurally fragile, and much effort has been devoted to improve their stability. The tubules from diblock copolymers would obviously avoid these problems because of their much greater stability. Until now, it has been possible to prepare long tubules only from polystyrene-*b*-poly(ethylene oxide) (PS-*b*-PEO) diblock copolymers.¹⁴ Now it is found that tubules can also be obtained occasionally from PS₂₀₀-*b*-PAA₁₈ diblocks in a mixture of DMF and dioxane. Figure 7 shows a typical example of tubules which were obtained when a mixture of DMF and dioxane at a 1:1 weight ratio was used as the common solvent. The tubules have a wall thickness of *ca.* 20 nm and an outside diameter of *ca.* 100 nm and are many micrometers in length.

3.3. Polymer-Solvent Interactions. The results described above clearly show that the nature of the common solvent has a major effect on the morphology of the aggregates. It is obvious that for an amphiphilic PS-*b*-PAA copolymer, the interaction between the polymer chains and the solvent will influence the dimensions of both the aggregate core and the corona.

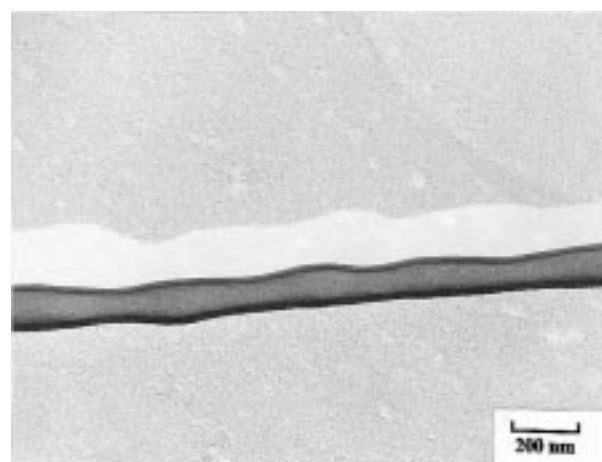


Figure 7. Tubular morphology of PS₂₀₀-*b*-PAA₁₈ crew-cut aggregates made from a mixture of DMF and dioxane (50/50, w/w). The initial polymer concentration was 0.5 wt %.

Generally, the strength of the polymer-solvent interaction is reflected by the χ parameter, which is related to the solubility parameter (δ) and the dielectric constant (ϵ). PS is a nonpolar polymer and the miscibility of PS and a solvent can be estimated to some extent from the solubility parameters of the PS and the solvent. As shown in Table 3, the solubility parameter of THF ($\delta = 18.6$ [MPa]^{1/2}) is closest to that of homo-PS ($\delta = 16.6$ – 20.2 [MPa]^{1/2}); the solubility parameter of dioxane ($\delta = 20.5$ [MPa]^{1/2}) is closer to that of polystyrene than that of DMF ($\delta = 24.8$ [MPa]^{1/2}). Therefore, within this simple approach, the strength of the PS-solvent interaction should be highest in THF, lower in dioxane, and lowest in DMF. From Figure 1, it is clear that the cwc value of homo-PS is highest in THF and lowest in DMF

Table 3. Some Physical Parameters of Solvents and Polymers

materials	solubility parameter (δ) ²⁷ [MPa] ^{1/2}	dielectric constant (ϵ) ²⁸
DMF	24.8	38.2
dioxane	20.5	2.2
THF	18.6	7.5
PS	16.6–20.2	
styrene	19.0	
PAA		
acrylic acid	24.6	
H ₂ O	47.9	80.1

(i.e., a much higher water content is needed to precipitate polystyrene in THF solution than in DMF solution). This trend reflects the differences of solubility parameters between the solvents and polystyrene. It is interesting to note that the actual δ parameter values calculated for the solvent mixtures at the cwc shown in Figure 1 are fairly close ($\delta = 26.0$, 23.5, and 23.9 [MPa]^{1/2} for the mixtures of H₂O with DMF, dioxane and THF, respectively). It is not surprising, therefore, that the micellization of the block copolymers is induced in these mixtures at that point. On the other hand, since PAA is polar, the strength of the PAA–solvent interaction should be related to the polarity of the solvent. The polarity of DMF is highest ($\epsilon = 38.2$); the polarity of THF is lower ($\epsilon = 7.5$); that of dioxane is lowest ($\epsilon = 2.2$). Therefore, the interaction between PAA and DMF should be the strongest and that between PAA and dioxane is the weakest. All these factors must be considered when we discuss the morphogenic effect of the solvent.

3.3.1. Solvent Content in the PS. As suggested by Nagarajan,²³ we found experimentally that changing the solvent content of the core can change the aggregate morphology. However, changing the solvent can change not only the core dimensions but possibly also the repulsion between corona chains, particularly when the corona chains are ionizable or ionic, and the dielectric constant of the solvent changes because of changes in the composition. As will be shown below, the solvent content in the PS aggregate core depends on both the nature of the common solvent and the water content.

Since the major component of the PS-*b*-PAA copolymer is polystyrene, it is useful to explore the effect of water on homopolystyrene (homo-PS) solutions. This will reflect the behavior of the PS core in the aggregates. The measurement of the solvent content in the PS-rich phase of a phase-separated ternary system of PS, common solvent, and water has been described in the Experimental Section. Figure 8 presents the experimental curves for the solvent content in the PS-rich phase as a function of water content (the insert shows the solvent content as a function of the water increment beyond the cwc). At the onset of microphase separation, the solvent content in the PS-rich phase is highest in THF, followed by dioxane and DMF. In each solution, the solvent content in the PS-rich phase decreases as the water content increases. As the solvent content in the PS-rich phase decreases, the viscosity of that phase increases. Therefore, the measurement of the solvent content by this method cannot extend to a high water content range. Figure 8 also shows that the drop in the solvent content in the PS-rich phase with increasing water content is much less steep in THF than in dioxane or DMF. This suggests that the effect of water content in the solution on the solvent content in the PS-rich phase is weaker in THF than in DMF or in dioxane.

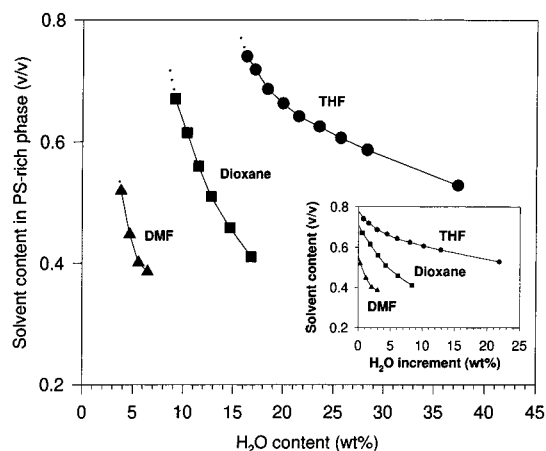


Figure 8. Solvent content in the PS-rich phase as a function of the water content (dotted lines extrapolate to the cwc). The insert shows the plot against the water increment beyond the cwc.

This trend parallels the effect of water on the degree of micellization (see Figure 4). The underlying reason for this behavior is the stronger interaction between the PS block and the THF vs that in dioxane or DMF, so that more water is needed to remove the solvent from the PS-rich phase in THF than in the other two solvent systems.

3.3.2. Degree of Stretching of the PS in Aggregate Core. In contrast to PS homopolymer solutions, where the polymer chains aggregate, phase separate, and settle at the bottom of the solutions, the colloidal solutions of PS-*b*-PAA diblock copolymers are stable, even after the water content exceeds the cwc, because of micellization. Therefore, experiments similar to those described above for the homopolymer cannot be performed, and much more sophisticated studies would have to be undertaken. However, it is expected that the solvent content in the PS-*b*-PAA aggregate cores as a function of water content in the solvent should parallel that in the PS homopolymer. When water is added beyond a certain point, the structures of the aggregates become locked because the mobility of the polymer chains is reduced to a very low level. However, after the isolation into water and subsequent drying, the dimension of the aggregate core is expected to be smaller than the corresponding value at the moment of the structural freezing of the aggregates.

It seems reasonable to suggest that the average degree of stretching of the PS chains increases with an increase of the solvent content in the aggregate cores. This stretching is entropically unfavorable. As the degree of stretching increases, the high stretching penalty for the PS chains in the core changes the aggregate morphology progressively from a sphere to a cylinder, or to a bilayer in order to decrease the overall free energy of micellization.¹²

The size of the core and therefore also the degree of the stretching of the PS chains (S_c) is also related to the repulsive interaction among the PAA corona chains. A decrease of the repulsion between corona chains will lead to an increase of the aggregation number; the dimension of the core must increase correspondingly, and therewith also the degree of stretching. Because the repulsive interactions among the PAA corona chains are related to the PAA–solvent interaction (i.e., the higher the strength of the PAA–solvent interaction, the higher the repulsion among the corona chains), the

Table 4. Some Characteristics of PS-*b*-PAA Aggregates in DMF, Dioxane, and THF (the Initial Polymer Concentration Was 2 wt %)

PS- <i>b</i> -PAA	PAA (mol %)	solvent	morphology	d^a (nm)	S_c^b
PS ₁₆₈ - <i>b</i> -PAA ₅₉	26.0	DMF	sphere	23	1.3
		dioxane	sphere	32	1.8
		THF	sphere	27	1.5
PS ₄₉₀ - <i>b</i> -PAA ₈₇	15.1	DMF	sphere	29	1.0
		dioxane	rod	57	1.9
		THF	sphere	42	1.4
PS ₅₀₀ - <i>b</i> -PAA ₅₈	10.4	DMF	sphere	30	1.0
		dioxane	vesicle	37	1.2
		THF	vesicle	50	1.6
PS ₃₉₀ - <i>b</i> -PAA ₄₁	9.5	DMF	sphere	32	1.2
		dioxane	vesicle	39	1.4
		THF	vesicle	45	1.7

^a Average diameter of the spherical and cylindrical micelles or wall thickness of the vesicles. ^b Degree of stretching of the PS blocks; for spheres or cylinders, it is defined as a ratio of the radius to the end-to-end distance of the PS block in the unperturbed state; for vesicles, half of the wall thickness is used.

degree of stretching in the core is also related to the PAA-solvent interaction. While the PS-solvent and the PAA-solvent interactions have opposite effects on the degree of the stretching (in the case of dioxane and THF), the overall S_c values must depend on the relative importance of each contribution. This aspect of the aggregate formation can be illustrated by discussing the results presented in Table 4.

Table 4 lists some structural parameters of several PS-*b*-PAA aggregates. The degree of stretching of the PS in the core (S_c) is defined as the ratio of the micelle core radius (R_{core}) to the end-to-end distance of the PS chain in the unperturbed state (R_0).¹² The micelle core radius is measured from the TEM pictures, and an average value is taken. The end-to-end distance of the PS chains in the unperturbed state is given by²⁷

$$R_0 \text{ (nm)} = 0.067M^{1/2}$$

where M (g/mol) is the molecular weight of the polystyrene block and the value 0.067 applies to various solvents.

PS₁₆₈-*b*-PAA₅₉ has a relatively high PAA content (26.0 mol % PAA) and yields only spherical aggregates of a narrow size distribution in all the solvents used in this work. However, the core radii of the aggregates prepared in the various solvents are different. The R_{core} of the spheres in dioxane is highest, and that in DMF is smallest, which means that the S_c value is highest in dioxane and smallest in DMF. For this polymer, the PAA-solvent interaction dominates the free energy of micellization. From the polarity of the solvent, it is apparent that the repulsive interactions between the PAA corona chains are weakest in dioxane, stronger in THF, and strongest in DMF. The increase of the repulsive interaction among the corona chains results in a decrease of the aggregation number which, in turn, decreases the dimension of the core and the degree of the stretching of the PS chains. Therefore, according to the strength of the PAA-solvent interaction (neglecting the effect of PS-solvent interaction in the core), the order of S_c in the three solvents is expected to be

$$\text{dioxane} > \text{THF} > \text{DMF}$$

which agrees with the experimental finding.

In PS₄₉₀-*b*-PAA₈₇, the PS and PAA blocks are longer than those in PS₁₆₈-*b*-PAA₅₉, but the PAA content is lower (only 15.1 vs 26.0 mol %). The aggregate morphologies in THF and DMF are still spherical, while cylinders are formed in dioxane. Thus, the PAA-solvent interaction still appears to be dominant, with the PAA length shorter in dioxane than in THF or DMF. Therefore, it appears that in dioxane the radius for the hypothetical sphere has increased to the point where the degree of stretching in the core has crossed the sphere/rod morphological boundary and rods are formed. Even though S_c is still high, it is lower than it would be for a sphere.

The PAA contents in PS₅₀₀-*b*-PAA₅₈ and PS₃₉₀-*b*-PAA₄₁ are still lower (10.4 and 9.5 mol %) than those in PS₁₆₈-*b*-PAA₅₉ and PS₄₉₀-*b*-PAA₈₇. These polymers still yield only spherical aggregates in DMF, but give vesicles in both THF and dioxane. Table 4 shows that the degree of stretching of the PS chains in the wall of the aggregates for these samples is higher in THF than in dioxane and smallest in DMF. Thus, in DMF the spherical morphology is maintained. In THF and dioxane, however, the chain stretching in the core has resulted in two morphological steps beyond spheres, all the way to vesicles. But even here, the S_c values are still high. When the PAA content decreases further to the range of 7.1–5.8 mol % (see Table 2), large compound micelles (LCMs) are first seen in THF, while vesicles are still the dominant morphology in dioxane and spheres in DMF.

Because the strength of the PAA-DMF interaction is stronger than those of PAA-THF and PAA-dioxane, and the strength of the PS-DMF interaction is weaker than those of PS-THF and PS-dioxane, the dimension of the PAA corona is larger and the dimension of the PS core is smaller in DMF than in THF or dioxane. Therefore, spherical micelles are favored in DMF relative to THF or dioxane. When the aggregates made from THF and dioxane are compared, the situation is more complicated. From a consideration of the PAA-solvent interactions alone, the PAA-dioxane interaction is weaker than that between PAA and THF; thus, the size of the PAA corona should be smaller in dioxane than in THF. Therefore, LCMs are expected to appear first in dioxane instead of in THF. Since LCMs are seen first in THF, it means that another interaction (i.e., the PS-solvent interaction) has now become more important. From a consideration of the PS-solvent interaction alone, the strength of the PS-THF interaction is higher than that of the PS-dioxane interaction. Therefore, the core dimension, and in turn, the degree of stretching of PS in the cores, is larger in THF than in dioxane. Therefore LCMs would be expected to appear first in THF, which is, indeed, found experimentally. Eventually, when the PAA content in the PS-*b*-PAA diblock copolymer is very low (4.8 mol % of PAA), the large compound micelle morphology is the only one to be observed in both THF and dioxane, while spheres are still observed in DMF. These results demonstrate that as the PAA content decreases, the importance of the PAA-solvent interaction for the free energy of micellization decreases while that of the PS-solvent interaction increases. Therefore, the solvent content in the aggregate cores, which is related to the PS-solvent interaction, becomes gradually the major factor affecting the structure of the aggregates.

Table 5. Some Characteristics of Aggregates Made from an Identical PS₂₀₀-*b*-PAA₁₈ Diblock in Various Mixtures of DMF and THF (the Initial Polymer Concentration was 0.5 wt %)

THF content (wt%)	morphology	d ^a (nm)	S _c ^b
0	sphere	30	1.6
5	cylinder	27	1.4
10	lamella and vesicle	23	1.2
25	vesicle	29	1.5
40	vesicle	30	1.6
50	vesicle	36	1.9
67	vesicle	39	2.0

^{a,b} Have the same meaning as in Table 4.

In section 3.2.3, it has been reported that the morphology of the aggregates made from PS₂₀₀-*b*-PAA₁₈ at a concentration of 0.5 wt % changes progressively from spheres to large compound micelles as the initial solvent changes from DMF, to a mixture of DMF/THF in various ratios, and then to THF. Table 5 presents the structural parameters of these aggregates. When the THF content increases from 0 to 10 wt %, the morphology of the aggregates changes from the spheres to cylinders and to a mixture of lamellae and vesicles. These morphological changes can be explained by a progressive increase of the dimension of the PS core accompanied by a slight decrease of the dimensions of the PAA corona when the THF content increases. The repulsion among the corona chains of PS₂₀₀-*b*-PAA₁₈ crew-cut aggregates is believed to change relatively little in a mixture of DMF and THF of different ratios because the PAA is, at best, only very slightly ionized in these solvents and the PAA length is quite short. However, the core dimension, as well as the degree of stretching of PS chains in the core, probably increases considerably as the THF/DMF ratio increases. Actually, it is possible that the local THF/DMF ratio in the core domain is higher than the overall ratio, since the strength of the PS-THF interaction is higher than that of the PS-DMF interaction, which might lead to an enrichment of the THF in the core. This might be a reason the small increase in the THF content, in the range of 0–10 wt %, results in a change of the aggregate morphology by two steps (sphere → rod → vesicle).

It has been reported previously¹² that the degree of stretching decreases as the morphology changes from the spheres to cylinders and to vesicles, because the additional degree of freedom along the axis or the plane allows many chains in the cylinders or the bilayers to be incorporated into the structure without significant changes in their conformation. This is also found to be the case in the present study. However, when the THF content increases further to the range of 25–67 wt %, where vesicles are the predominant morphology, the degree of stretching of the PS chains in the wall of the aggregates increases with increasing THF content. In these cases, the increase of the solvent content in the aggregates is most likely responsible for the increase of the degree of stretching of the PS in the wall along with increasing THF content, while the morphology stays the same. No morphological boundaries are crossed, so the wall thickness increases monotonically.

In summary, the degree of the stretching of the PS chains in the aggregate cores is related to both the PS-solvent and the PAA-solvent interactions. In terms of the strength of the PS-solvent interaction, the S_c has the order of THF > dioxane > DMF. In terms of the

strength of the PAA-solvent interaction, the order is dioxane > THF > DMF. In both cases, the S_c value in DMF is always lowest; however, the order in THF and in dioxane is reversed. The relative importance of these two interactions is related to the PAA content in the PS-*b*-PAA diblock. The higher the PAA content, the more important the PAA-solvent interaction.

4. Conclusions

The morphogenic effect of solvent on the crew-cut aggregates of polystyrene-*b*-poly(acrylic acid) (PS-*b*-PAA) diblock copolymers has been explored. The morphologies and structural parameters of the PS-*b*-PAA aggregates are related to two major factors (i.e., the PS-solvent interaction, which determines the solvent content and the degree of stretching of PS chains in the cores, and the PAA-solvent interaction, which determines the repulsion among the corona chains).

The critical water content, cwc, at which micellization of the PS blocks starts, is related to the nature of the common solvent. The stronger the PS-solvent interaction, the higher the cwc. Therefore, the cwc is highest in THF, followed by dioxane and DMF. The relationships between the cwc and the logarithm of the polymer concentration in the various solvents is linear. For PS-*b*-PAA diblock copolymers in DMF or dioxane, the micelle fraction as a function of water content increases very rapidly relative to that in THF.

The same PS-*b*-PAA diblock can yield various aggregates in different solvents. When a mixture of two solvents is used, the degree of morphological control of the aggregates improves. The stronger the PS-solvent interaction (i.e., the smaller difference of the solubility parameter between the PS and the solvent), the higher the degree of stretching of the PS in the cores. Since the high degree of stretching is entropically unfavorable, the morphology of the aggregates can change in order to decrease the free energy of micellization. When a solvent of low dielectric constant (e.g., dioxane) is used, the repulsive interaction among the PAA corona chains is low, which will increase the aggregation number relative to that in a solvent of high dielectric constant (e.g., DMF). As a result, the degree of the stretching of the PS increases correspondingly. Obviously, the PAA-solvent interaction is more important as the PAA content increases; similarly, the PS-solvent interaction is relatively more important as the PAA content decreases. The final morphologies reflect a balance of these interactions.

Acknowledgment. The authors thank The Natural Sciences and Engineering Research Council of Canada (NSERC) for financial support of this research.

References and Notes

- (1) Price, C. In *Developments in Block Copolymers*; Goodman, I., Ed.; Applied Science Publishers: London, 1982; Vol. 1, p 39.
- (2) Selb, J.; Gallot, Y. In *Developments in Block Copolymers*; Goodman, I., Ed.; Applied Science Publishers: London, 1985; Vol. 2, p 27.
- (3) Tuzar, Z.; Kratochvil, P. In *Surface and Colloid Science*; Matijevic, E., Ed.; Plenum Press: New York, 1993; Vol. 15, p 1.
- (4) Xu, R.; Winnik, M. A. *Macromolecules* **1991**, *24*, 87.
- (5) Wilhelm, M.; Zhao, C. L.; Wang, Y.; Xu, R.; Winnik, M. A. *Macromolecules* **1991**, *24*, 1033.
- (6) Prochazka, K.; Kiserow, D.; Ramireddy, C.; Tuzar, Z.; Munk, P.; Webber, S. E. *Macromolecules* **1992**, *25*, 454.

- (7) Tuzar, Z.; Kratochvil, P.; Prochazka, K.; Munk, P. *Collect. Czech. Chem. Commun.* **1993**, *58*, 2362.
- (8) Astafieva, I.; Zhong, X. F.; Eisenberg, A. *Macromolecules* **1993**, *26*, 7339.
- (9) Qin, A.; Tian, M.; Ramireddy, C.; Webber, S. E.; Munk, P. *Macromolecules* **1994**, *27*, 120.
- (10) Gao, Z.; Varshney, S. K.; Wong, S.; Eisenberg, A. *Macromolecules* **1994**, *27*, 7923.
- (11) Zhang, L.; Barlow, R. J.; Eisenberg, A. *Macromolecules* **1995**, *28*, 6055.
- (12) (a) Zhang, L.; Eisenberg, A. *Science* **1995**, *268*, 1728. (b) Zhang, L.; Eisenberg, A. *J. Am. Chem. Soc.* **1996**, *118*, 3168.
- (13) (a) Zhang, L.; Yu, K.; Eisenberg, A. *Science* **1996**, *272*, 1777. (b) Zhang, L.; Eisenberg, A. *Macromolecules* **1996**, *29*, 8805.
- (14) (a) Yu, K.; Eisenberg, A. *Macromolecules* **1996**, *29*, 6359. (b) Yu, K.; Zhang, L.; Eisenberg, A. *Langmuir* **1996**, *12*, 5980.
- (15) Yu, Y.; Zhang, L.; Eisenberg, A. *Langmuir* **1997**, *13*, 2578.
- (16) Zhang, L.; Eisenberg, A. *Macromol. Symp.* **1997**, *113*, 221.
- (17) Zhang, L.; Shen, H.; Eisenberg, A. *Macromolecules* **1997**, *30*, 1001.
- (18) Shen, H.; Zhang, L.; Eisenberg, A. *J. Phys. Chem.* **1997**, *101*, 4697.
- (19) (a) Desjardins, A.; Eisenberg, A. *Macromolecules* **1991**, *24*, 5779. (b) Desjardins, A.; Van de Ven, T. G. M.; Eisenberg, A. *Macromolecules* **1992**, *25*, 2412. (c) Gao, Z.; Desjardins, A.; Eisenberg, A. *Macromolecules* **1992**, *25*, 1300.
- (20) Honda, C.; Sakaki, K.; Nose, T. *Polymer* **1994**, *35*, 5309.
- (21) (a) Spatz, J. P.; Mössmer, S.; Möller, M. *Angew. Chem., Int. Ed. Engl.* **1996**, *35* (13) 1510. (b) Spatz, J. P.; Sheiko, S.; Möller, M. *Macromolecules* **1996**, *29*, 3220.
- (22) Ding, J.; Liu, G. *Macromolecules* **1997**, *30*, 655.
- (23) Nagarajan, R. In *Solvents and Self-organization of Polymers*; Webber, S. E., Munk, P., Tuzar, Z., Eds.; NATO ASI Series E.; Kluwer Academic Publishing: Dordrecht, 1996; Vol. 327, p 121.
- (24) Yu, Y.; Eisenberg, A. *J. Am. Chem. Soc.* **1997**, *119*, 8383.
- (25) Hautekeer, J. P.; Varshney, S. K.; Fayt, R.; Jacobs, C.; Jerome, R.; Teyssie, Ph. *Macromolecules* **1990**, *23*, 3893.
- (26) Zhong, X. F.; Varshney, S. K.; Eisenberg, A. *Macromolecules* **1992**, *25*, 7160.
- (27) Brandrup, J.; Immergut, E. H. *Polymer Handbook*, 3rd ed.; Wiley-Interscience: New York, 1989; VII 526, VII 38.
- (28) Lide, D. R. *CRC Handbook of Chemistry and Physics*, 78th Ed.; CRC Press: New York, 1997–1998; p 6–139.

MA971254G